



Deciphering the molecular mechanism of long non-coding RNA HIF1A-AS1 regulating pancreatic cancer cells

Jiaxin Zhang, PhD^{a,*}, Yifeng Sun, MD^b, Jiahui Ma, MD^c, Xiang Guo, MD^c

Background: *HIF1A-AS1*, an antisense transcript of *HIF1 α* gene, is a 652-bp lncRNA that is globally expressed in multiple tissues of animals. Recent evidence indicated that *HIF1A-AS1* was involved in tumorigenesis of several types of cancer. However, the role of lncRNA in PC has not been reported, and the molecular mechanism remains elusive.

Results: In order to investigate the role of *HIF1A-AS1* in PC, it was overexpressed in some PC cell lines (PANC-1, PATU8988 and SW1990), and a series of experiments including cell viability detection, flow cytometry, transwell migration, clone formation and wound healing were performed. Functionally, the results indicated that overexpression of *HIF1A-AS1* could greatly inhibit proliferation and migration and promote apoptosis of PC cells. Moreover, the isobaric tags for relative and absolute quantification (iTRAQ) quantitative proteomics analysis was implemented to explore the underlying mechanism and the results indicated that OE of *HIF1A-AS1* globally affected the expression levels of multiple proteins associated with metabolism of cancer. At last, the network analysis revealed that most of these differentially expressed proteins (DEPs) were integrated and severed essential roles in regulatory function. In view of this, we guessed *HIF1A-AS1* overexpression induced the dysfunction of metabolism and disordered proteins' translation, which may account for its excellent tumour suppressor effect.

Conclusions: *HIF1A-AS1* altered the cell function of PC cell lines via affecting the expression of numerous proteins. In summary, *HIF1A-AS1* may exhibit a potential therapeutic effect on PC, and our study provided useful information in this field.

Keywords: HIF1A-AS1, long non-coding RNA, molecular mechanism, pancreatic cancer, restrain

Introduction

Pancreatic cancer (PC) remains one of the most common causes of cancer-related mortality^[1] at the seventh in humans worldwide^[2], with 5-year overall survival rate of less than 5%^[3]. In most cases, PC develops and is usually clinically silent at the early stage, but the variable symptoms, local invasiveness, or metastases only develop at an advanced stage^[4]. Nowadays, the therapeutic efficacy of PC is still very limited and far from satisfactory^[5,6]. Hence, in order to enhance the cure rate of PC, it

^aSchool of Physical Education, Xinxiang Medical University, Xinxiang, Henan,

^bDepartment of Occupational Health and Occupational Disease, School of Public Health, Zhengzhou University, Zhengzhou and ^cZhengzhou Central Hospital Affiliated to Zhengzhou University, Xinxiang Medical University, Xinxiang, Henan, China

J.Z. is both the first and corresponding author.

Sponsorships or competing interests that may be relevant to content are disclosed at the end of this article.

*Corresponding author. Address: Community Health Center, Zhengzhou, China. Tel.: +86 155 382 35999. E-mail: misscrystal2020@163.com (J. Zhang).

Copyright © 2024 The Author(s). Published by Wolters Kluwer Health, Inc. This is an open access article distributed under the terms of the Creative Commons Attribution-Non Commercial-No Derivatives License 4.0 (CCBY-NC-ND), where it is permissible to download and share the work provided it is properly cited. The work cannot be changed in any way or used commercially without permission from the journal.

Annals of Medicine & Surgery (2024) 86:3367–3377

Received 25 January 2024; Accepted 11 April 2024

Supplemental Digital Content is available for this article. Direct URL citations are provided in the HTML and PDF versions of this article on the journal's website, www.lww.com/annals-of-medicine-and-surgery.

Published online 29 April 2024

<http://dx.doi.org/10.1097/MS9.0000000000002097>

HIGHLIGHTS

- In order to investigate whether the *HIF1A-AS1* could mediate the pancreatic cancer (PC) or not, it were overexpressed in some PC cell lines (PANC-1, PATU8988 and SW1990), and a series of experiments including cell viability detection, flow cytometry, transwell migration, clone formation and wound healing were performed. Functionally, the results indicated that overexpression of *HIF1A-AS1* could inhibit proliferation and shift, and promote apoptosis of PC cells.
- To explore underlying molecular mechanism of anti-tumorigenic actions of *HIF1A-AS1* in PC cells, the isobaric tags for relative and absolute quantification (iTRAQ) quantitative proteomics analysis was implemented and the results indicated that OE of *HIF1A-AS1* globally affected the expression levels of multiple proteins associated with the metabolism of cancer.
- *HIF1A-AS1* altered the cell function of PC cell lines via affecting the expression of numerous proteins. In summary, *HIF1A-AS1* may be useful for the early diagnosis of PC, and our study provided useful information in this field.

is necessary to investigate the molecular mechanisms, which would provide new opportunities to improve effective therapeutic strategies against PC.

Long non-coding RNAs (lncRNAs), a kind of non-coding RNAs transcripts, comprise longer than 200 bp without protein-coding potential^[7–9]. Current studies have shown that lncRNAs could mediate gene expression via chromosome remodelling,

transcription and post-transcriptional processes^[10]. As so far, increasing evidences demonstrate that lncRNAs play an important role in regulating vital molecular mechanisms^[11] and biological functions of the cells^[12,13], such as proliferation, migration, invasion, cell cycle and apoptosis^[14–16]. Without a doubt, various expressions of lncRNAs could contribute to tumour development and progression^[17], but its regulatory mechanism have not been completely investigated.

HIF1A-AS1 is an antisense transcript of *HIF1 α* ^[18]. Accumulating evidences have revealed that it plays a key role in the proliferation and apoptosis of vascular smooth muscle cells^[19–21], and human hepatic stellate cells^[22]. Furthermore, it promotes tumour necrosis factor- α -induced apoptosis^[23], thereby affecting the occurrence and development of thoracic aortic aneurysm^[24]. *HIF1A-AS1* can regulate starvation-induced hepatocellular carcinoma cell apoptosis, promoting hepatocellular carcinoma (HCC) cell progression^[25]. Therefore, *HIF1A-AS1* has the capacity to affect the occurrence and development of multiple types of cancer, but there is no report on the molecular regulation mechanism of *HIF1A-AS1* in PC.

In the current study, to explore the role of *HIF1A-AS1* in PC not, we constructed overexpression (OE) plasmids containing *HIF1A-AS1*, and transferred them to several PC cell lines (PANC-1, PATU8988 and SW1990). It was observed that *HIF1A-AS1* greatly inhibited proliferation and migration, while markedly facilitated apoptosis of PC cells. The above pieces of evidence emphasized the suppressed effect of *HIF1A-AS1* on pancreatic cancer. Proteomics demonstrated *HIF1A-AS1* altered the cell function of PC cell lines via affecting the expression of 338 proteins. Finally, the results of bioinformatics analysis revealed most up-regulated DEPs were enriched in “RNA transport” (ID: ko03013) and “Metabolic pathways” (ID: ko01100), while the down-regulated DEPs were mainly enriched in “Metabolic pathways” (ID: ko01100) and “Protein processing in endoplasmic reticulum” (ID: ko04141). In view of this, we guessed *HIF1A-AS1* overexpression induced the dysfunction of metabolism and disordered proteins’ translation, which may account for its excellent tumour suppressor effect. The results of proteomics revealed a large number (338) of differentially expressed proteins (DEPs), which may contribute to the anti-tumours effect of this lncRNA. Here, we report the results.

Materials and methods

Cell culture

The human pancreatic cancer cell lines (PANC-1, PATU8988 and SW1990) and one normal cell line (HPDE6-C7) were provided by Procell (Wuhan, China). The cells were cultured in monolayers in Dulbecco’s modified Eagle’s medium (DMEM) (Invitrogen), which were supplemented with 10% foetal bovine serum (Hyclone UT), 100 U/ml penicillin and 50 μ g/m streptomycin (Beyotime) under a 95% humidified atmosphere and 5% CO₂ at 37°C.

Plasmid construction, lentivirus package and transfection

HIF1A-AS1 was cloned into the pcDNA3.1(+) vector at *KpnI* (GGTACC) and *XbaI* (CTCGAG). Two micrograms of plasmids containing *HIF1A-AS1* were mixed with the lentivirus packaging plasmids pMDLg-pRRE, pMD2.G, and pRSV-Rev according to

the previous standard protocol^[26]. Subsequently, PC cells were infected with 20 multiplicity of infection (MOI) lentivirus for 24 h and incubated in a fresh medium. The cells were washed with fresh complete media after 24 h, and the efficiency OE of *HIF1A-AS1* was verified by quantitative real-time polymerase chain reaction (qRT-PCR).

RNA extraction and qRT-PCR

Total RNA was extracted from the cells using TRIzol reagent (Ambion) and further purified with two phenol-chloroform treatments, then treated with RQ1 DNase (Promega) to digest DNA. The purified RNAs were determined using a Nano Photometer spectrometer at 260/280 nm and next verified by 1.2% agarose gel electrophoresis. The cDNA was synthesized with random primers using the High-capacity cDNA Reverse-Transcription Kit (Takara), and real-time PCR was applied to detect gene expressions. The primers, which were designed by Primer 5 software, were listed in Table S1, Supplemental Digital Content 1, <http://links.lww.com/MS9/A444> with SYBR Green I dye (Qiagen, Hilden, Germany). The PCR conditions were as follows: pre-denaturation at 95°C for 1 min, 40 cycles of denaturing at 95°C for 15 s, annealing at 60°C for 30 s and elongation at 72°C for 40 s. The relative expression of genes was analyzed by the $2^{-\Delta\Delta CT}$ method with the *Actin* as an internal control^[27].

Cell viability detection

The viability of PC cell was measured by the Cell Counting Kit-8 (CCK-8) assay (Solarbio) according to the manufacturer’s instructions. The cells were slightly seeded into the 96-well plates with 100 μ l suspension per well overnight. At 0, 24, 48 and 72 h, 10 μ l of CCK-8 solution was added to each well, and then the plates were incubated for 0.5 h. At last, absorbance was measured at 450 nm by microplate reader (Bio-Rad).

Flow cytometric detection

The number of apoptotic cells was counted by flow cytometry with Annexin V-conjugated FITC Apoptosis detection kit (BD). After infecting for 24 h, cells were harvested and washed twice with PBS, then re-suspended in the mixed solution which contained FITC-conjugated anti-Annexin V antibody and Propidium iodide (PI). Apoptosis was detected with a Fluorescence Activating Cell Sorter (FACS) calibur flow cytometer MoFLO XDP (Beckman).

Transwell invasion

For the transwell assay, the properties of migration of cells were measured by 24-well transwell plates (Corning). About 1×10^4 cells per well were seeded into the upper chamber with serum-free medium in triplicate. Medium containing 10% FBS (300 μ l) was added to the DMEM under a 95% humidified atmosphere and 5% CO₂ at 37°C. After incubation for 24 h, the medium was removed, and cells were fixed with 4% paraformaldehyde for 15 min, then stained with 0.1% crystal violet for 20 min, and finally counted from five randomly chosen fields for each well by stereo microscope (Leica).

Wound-healing assay

Firstly, the transfected cells were seeded in 6-well plates. One hour later, confluent monolayers in each well were washed with PBS and then generated a wound by a 200 μ l sterile pipette tip. Wound healing was evaluated, and photographed images were taken by 200 \times a Zeiss microscope (Leica) from each well at 0, 24, and 48 h post-injury time points after the wound was made.

Cell clone formation assay

Prepared cells were plated into six-well plates (800 cells per well) and cultured for 12 days, then digested at the logarithmic phase to generate a single-cell suspension using a culture medium. Cells were stained with 0.4% crystal violet (Bio Basic Inc., Mark-ham, Canada). The inverted microscope (Leica, Wetzlar, Germany) has been exploited for calculating the number of colonies.

Western blotting analysis

PC cells were collected and the homogenates were centrifuged for 30 min at 4°C, 12 000 rpm with cell lysis buffer. Then the protein extracts were separated on 10% SDS-PAGE and soon transferred to polyvinylidene difluoride (PVDF) membranes. Membranes were incubated at room temperature for 1 h in a 5% skim milk TBST blocking solution and agitated with specific primary antibodies anti-GAPDH (Beyotime), anti-Bax (Cell signaling technology), anti-P53 (Szybio), anti- the full-length Caspase-3 (Cell Signaling Technology), and anti- the full-length PARP1 (Cell Signaling Technology) at 4°C overnight. Next, membranes were incubated with secondary antibodies conjugated by horseradish peroxidase (HRP) (Zhong san jinqiao) for 50 min at room temperature. At last, protein bands were determined by the Western blotting detection system (GE Healthcare).

iTRAQ quantitative proteomics analysis

First, we extracted proteins from prepared cells. Briefly, the lysis buffer (7M Urea/2M Thiourea/4% SDS/40 mM Tris-HCl, pH 8.5), which contains 1 mM phenylmethanesulfonyl fluoride (PMSF) and 2 mM ethylenediaminetetraacetic acid (final concentration), was added to the cells. Then, mixed and incubated them in ice for 5 min. Subsequently, DL-Dithiothreitol (DTT) was added to a final concentration of 10 mM. The lysate was sonicated on ice for 20 min and centrifuged at 4°C, 13 000g for 25 min^[28]. The supernatant was mixed with four volumes of precooled acetone and incubated at -20°C overnight. After centrifugation, the protein pellets were air-dried and re-dissolved in 8M urea/100 mM triethylamine borane (TEAB) (pH=8.0). Protein samples were incubated with 10 mM DTT at 56°C for 35 min and alkylated with 50 mM iodoacetamide (IAM) in the dark at room temperature for 30 min. The supernatant was transferred to a new centrifuge tube, and the protein precipitation was performed by acetone precipitation. The protein pellet was re-dissolved in 8 M urea/100 mM TEAB (pH=8.0) solution, and DTT was added to a final concentration for 10 mM. Incubating the mixture for 25 min at 56°C. Subsequently, IAM was added to obtain a volume of 55 mM, and the alkylation reaction was carried out at room temperature for 40 min in the dark. The protein concentration was assessed using the Bradford method.

The 100 μ g proteins were digested under the role of trypsin in each sample. After diluting the protein solution with 100 mM TEAB for five times, trypsin was added by a mass ratio of 1:50

(trypsin: protein) overnight at 37°C. The peptides were desalted with C₁₈ column after enzymolysis, and the desalted peptides were vacuum freeze-dried.

The mass spectrometry data were collected and monitored by the Eksigent nanoLC system (SCIEX, USA), which was coupled to the TripleTOF 5600+ mass spectrometers. Samples were iTRAQ labelled as follows: NC-1, X1; NC-2, X2; NC-3, X3; OE-1, X4; OE-2, X5; and OE-3, X6. NC-1, NC-2 and NC-3 refers to 3 parallel groups of the empty vector-controlled normal control (NC) PANC-1 cells, the other OE-1, OE-2 and OE-3 refers to 3 parallel groups of the same *HIF1A-AS1* overexpressed PANC-1 cells, and X1, X2, X3, X4, X5 and X6 refers to the order from sample 1–6. And all of them were mixed with equal amounts. Next, the polypeptide solution was added to analytical ChromXP C₁₈ column (Bonna-Agela Technologies Inc., Wilmington, DE) (5 μ m, 100 \AA , 4.6 \times 250 mm), and eluted at 300 nl/min on a C₁₈ analytical column (3 μ m, 75 μ m \times 150 mm) over 90 min gradient. The two mobile phases were buffer A (2% acetonitrile / 0.1% formic acid / 98% H₂O) and buffer B (98% acetonitrile / 0.1% formic acid / 2% H₂O), respectively. For Information Dependent Acquisition (IDA), the first-order mass spectrum was scanned with an ion accumulation for 250 ms, and the secondary mass spectrum of 30 product ion scans were collected with 50 ms. The MS1 spectrum was collected in the range 350–1500 m/z, and the MS2 spectrum was collected in the range 100–1500 m/z. Precursor ions were set from reselection for 15 s.

ProteinPilot Software v4.5 (AB Sciex) was implemented to monitor the original MS/MS file data. UniProt/SwissProt database was applied for database searching. The parameters were set as follows: the instrument was TripleTOF 5600+, iTRAQ quantification, and cysteine modified with IAM, and biological modifications were selected as ID focus, trypsin digestion, quantitate, bias correction, and background correction were used for protein quantification and normalization. For calculation of the false discovery rate (FDR), an automatic decoy database search strategy, the proteomics system performance evaluation pipeline software (PSPEP, integrated into the ProteinPilot Software), was resorted to estimate FDR. Unique peptides were implemented for iTRAQ labelling quantification, and peptides with global FDR values less than 1% were considered for further analysis. For proteins, whose quantitation is considerably different between OE and NC groups, a rigid standard of P less than 0.05 and $|\log_2(\text{fold change})| > 1.2$ was defined as differentially expressed proteins (DEPs).

Bioinformatics and annotations

The biological and functional properties of all the identified proteins were measured using NCBI nr (<http://www.ncbi.nlm.nih.gov/>) and Swiss-Prot/UniProt (<http://www.uniprot.org/>) databases, and were mapped with Gene Ontology (GO, <http://www.geneontology.org/>), the Cluster of Orthologous Groups of proteins (COGs, <http://www.ncbi.nlm.nih.gov/COG/>) databases and Kyoto Encyclopedia of Genes and Genomes (KEGG) (<http://www.genome.jp/kegg/>) databased, respectively. STRING v10.1 (<http://string-db.org/>) was applied to explore and analyze the protein-protein interaction (PPI) information of DEPs to evaluate the interactive associations. The PPI network was constructed and visualized by Cytoscape software (version 3.5.1; www.cytoscape.org).

Statistical analyses

All values were presented using the SPSS16.0 statistical software as the mean \pm standard deviation (SD). Statistically significant differences comparison between two groups means were determined by Student's *t*-test. *P* value less than 0.05 was considered to be statistically significant.

Data availability statement

The datasets generated and analyzed during the current study are available in the ProteomXchange repository (Accession No: IPX0003153000). For the interview, the datasets could also be obtained from a web link: <https://www.iprox.cn/page/PSV023.html?url=1632453584186C2vO>, with a code: Nvso.

Specific reporting guidelines

Cell line research

The human pancreatic cancer cell lines (PANC-1, PATU8988 and SW1990) and one normal cell line (HPDE6-C7) were provided by Procell (Wuhan, China).

Results

HIF1A-AS1 regulates the apoptosis and proliferation of PC cells

First of all, we measured the mRNA level of *HIF1A-AS1* in four kinds of pancreatic cells, including one normal cell line (HPDE6-C7) and three kinds of cancer cell lines (PANC-1, PATU8988 and SW1990). We found the mRNA expression of *HIF1A-AS1* was down-regulated in some PC cells compared with normal cell (Fig. S1D, Supplemental Digital Content 2, <http://links.lww.com/MS9/A445>). To investigate the role of *HIF1A-AS1* in PC cells, an OE vector containing the *HIF1A-AS1* was transfected into PANC-1 cells. The qRT-PCR experiment was applied to measure the efficiency of OE. The results showed that expression levels of *HIF1A-AS1* in OE cells was increased more than 10000 folds compared with the empty vector-controlled normal control (NC) cells (Fig. 1A), demonstrating a successful establishment of human PC cells with OE of *HIF1A-AS1*.

Some experiments, including CCK-8, were conducted to explore whether *HIF1A-AS1* regulates the proliferation of PC cells. The results indicated that viability cells with *HIF1A-AS1* OE was declined significantly during varying time periods (0, 24, 48 and 72 h) ($P < 0.001$) (Fig. 1B and C).

Furthermore, flow cytometry was used to count the apoptosis cells in OE and NC groups (Fig. 1D and E). It displayed that the OE of *HIF1A-AS1* significantly promoted apoptosis of PC cells, and the number of apoptotic cells obviously increased about 50% compared with the NC group (Fig. 1E). The above results indicated that *HIF1A-AS1* had the capacity to regulate proliferation and apoptosis of the PANC-1 cells. Further, western blot analysis reported that the expression of some apoptosis-related proteins, including caspase-3, Bax, P53 and PARP1, were facilitated in OE group (Fig. 1F).

To further verify this result, we also did the same experiment including CCK-8 in two other PC cell lines PATU8988 (Fig. S1A, Supplemental Digital Content 2, <http://links.lww.com/MS9/A445>, S2A and S2B, Supplemental Digital Content 3, <http://links.lww.com/MS9/A446>) and SW1990 (Fig. S1B, Supplemental Digital Content 2, <http://links.lww.com/MS9/A445>, S3A and S3B, Supplemental Digital Content 4, <http://links.lww.com/MS9/A447>). The results were consistent with that in PANC-1 cells. Therefore, all results indicated that OE of *HIF1A-AS1* inhibits proliferation and promotes apoptosis of the PC cells.

HIF1A-AS1 regulates the migration of PC cells

HIF1A-AS1 regulates the migration of PC cells

To further explore the role of *HIF1A-AS1* in regulating the migration of PANC-1 cells, transwell migration assays were performed. It showed that the migration ability of cells in OE groups was reduced about 50% ($P < 0.001$) (Fig. 2A and B). What's more, the relative clone formation efficiency decreased about 45% when *HIF1A-AS1* overexpressing, indicating a rather lower proliferative capacity (Fig. 2C and D). Cell migration was detected using a wound-healing assay in PANC-1 cells. The results from the invasion assay showed that OE of *HIF1A-AS1* promoted cell invasion after transfection for 24 and 48 h (Fig. 2E). And the difference in the wound width after 24 h of transfection is the most significant compared with the comparison exceeds the control by about 20% (Fig. 2F), suggesting a functional role for *HIF1A-AS1* in inhibiting migration of the PANC-1 cells.

In addition, similar experiments were carried out in two other cell lines (PATU8988 and SW1990). According to the analogous experimental results (Fig. S2C-H, Supplemental Digital Content 3, <http://links.lww.com/MS9/A446> and Fig. S3C-H, Supplemental Digital Content 4, <http://links.lww.com/MS9/A447>), it is further determined that *HIF1A-AS1* inhibits PC cell migration.

The summary of iTRAQ proteomics analysis

To explore the molecular mechanism of *HIF1A-AS1* mediating the proliferation, apoptosis and migration of PANC-1 cells, iTRAQ was applied to uncover altered protein expressions and signalling pathways.

In total, the quality of the data obtained from the iTRAQ was analyzed using parameters such as coefficient of variation about repeatability, distribution of unique peptide, peptide length, and distribution of coverage. First of all, for the repeatability, there is little difference in the concentration of CV data between NC and OE groups, and the cumulative percentages of CV were 7.81% and 7.29%, respectively, indicating that the PANC-1 samples in each group are more reproducible (Fig. 3A).

In accordance with the unique peptide determined as the peptide identified only for one protein, the presence of the corresponding protein can be uniquely determined. Then for the distribution of unique peptide number, the two-coordinate distribution map showed the number of unique peptides contained in all the proteins identified in this assay. For example, when the *x*-axis, left *y*-axis and right *y*-axis are 2, 646 and 26.25, respectively, it means that there are 646 proteins with 2 as the unique number of peptides, which account for 26.25% of the total number of proteins obtained (Fig. S4A, Supplemental Digital Content 5, <http://links.lww.com/MS9/A448>).

Subsequently, the length of the identified peptides was analyzed. The average length of the polypeptide was 11.56, which within a reasonable range. Moreover, the length of the identified peptides was mainly concentrated on 7–15 (Fig. S4B, Supplemental Digital Content 5, <http://links.lww.com/MS9/A448>). In addition, the protein identification coverage could reflect the overall accuracy of the identification results indirectly.

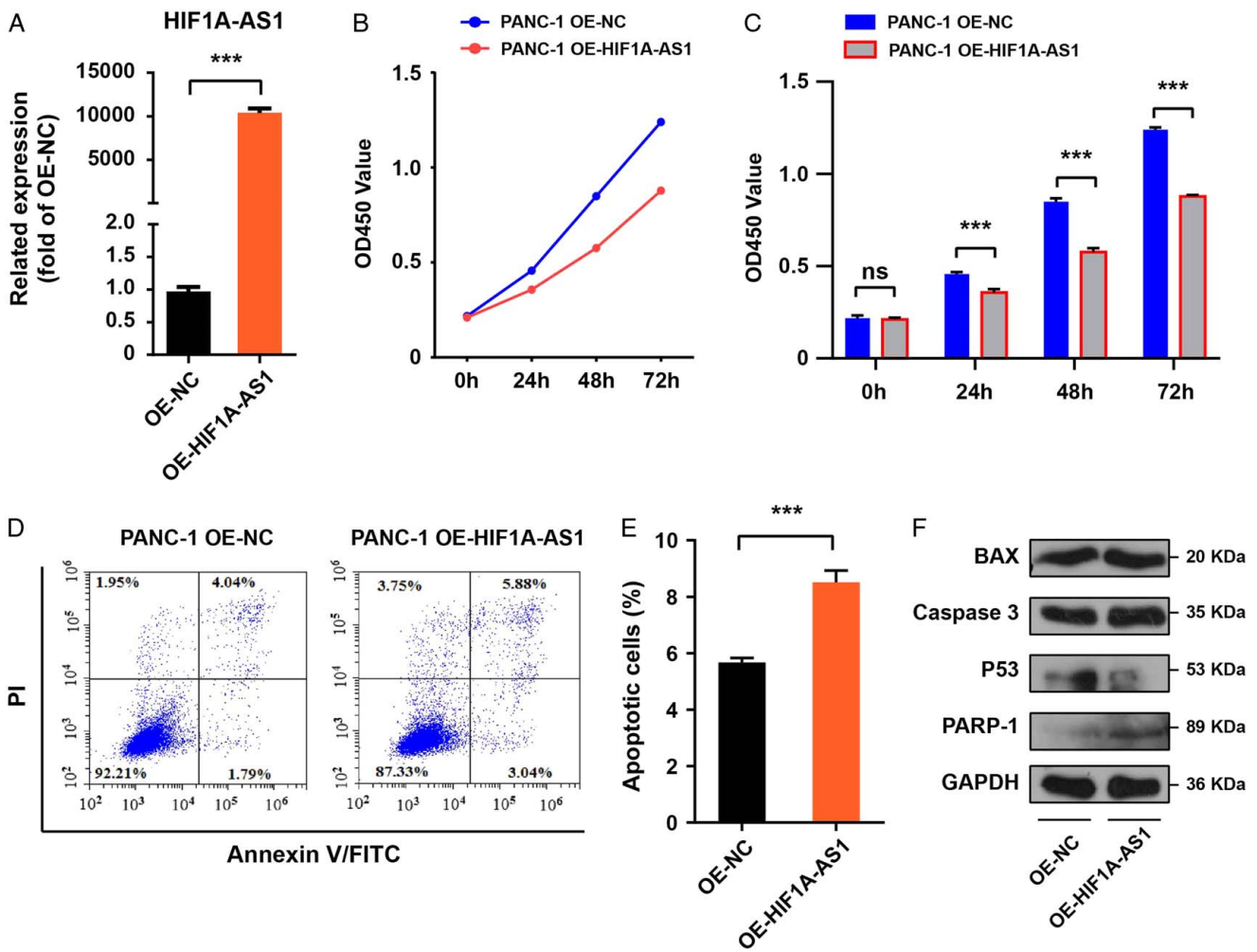


Figure 1. Overexpression (OE) of *HIF1A-AS1* affects the proliferation, apoptosis of the pancreatic cancer (PC) cells (PANC-1). (A) RT-qPCR measure the mRNA level of *HIF1A-AS1* in pancreatic cells (PANC-1), Real-time PCR showed that the levels of *HIF1A-AS1* was significantly increased in the cells from OE group compared with the empty vector-controlled normal control (NC) cells. (B, C) OE of *HIF1A-AS1* reduces significantly the viability of PANC-1 cells at 24, 48, and 72 h. (D) OE of *HIF1A-AS1* promotes significantly apoptosis of PANC-1 cells assessment of cellular apoptosis using Annexin V-fluorescein isothiocyanate staining coupled with flow cytometry. (E) Total percentage of apoptotic PANC-1 cells in each group are summarized with data presented as the mean \pm SD of three independent experiments. (F) Western blotting reveal the full length caspase-3, Bax, P53, and PARP1 protein expression in PANC-1 cells. *** $P < 0.001$. We used IMAGE J to analyze the expression of the target protein in western blot results. The specific data are as follows: (a) The protein expression increased about 22% for OE-Bax VS NC-Bax. (b) The protein expression increased about 20% for OE-caspase-3 VS NC-caspase-3. (c) The protein expression increased about 10% for OE-P53 VS NC-P53. (d) The protein expression increased about 34% for OE- PARP1 VS NC- PARP1.

The different coloured pie represented the percentage of proteins with different identification coverage ranges. It showed that 37.21% proteins were with the peptide coverage of less than 10%, and 39.51% proteins had more than or equal to 20% of peptide coverage, with the average protein identification coverage being 19.53% (Fig. S4C, Supplemental Digital Content 5, <http://links.lww.com/MS9/A448>).

A total of 4872 proteins were identified in all samples, and 4738, 2475 and 2539 ones were annotated successfully by GO, COG and KEGG, respectively (Fig. S4D, Supplemental Digital Content 5, <http://links.lww.com/MS9/A448>). Particularly, the GO enrichment for the 4738 annotated proteins was carried out, including cellular localization (CC) (Data not shown), molecular functions (MF) (Data not shown) and biological processes (BP). The BP classification showed that most of these proteins were enriched in the cellular process (13.04%), metabolic process

(11.26%), biological regulation (8.55%), regulation of biological process (8.13%), cellular component organization or biogenesis (7.00%) and so on (Fig. 3B).

Exploration of DEPs and functional analysis

On basis of the relative quantitative results, 338 DEPs were found in OE vs. NC by setting a rigid threshold ($FC \geq 1.2$ or ≤ 0.83 , $P \leq 0.05$), and the number of up-regulated and down-regulated DEPs were 183 and 155 (Table S2, Supplemental Digital Content 6, <http://links.lww.com/MS9/A449>), respectively. The protein abundance distribution graph and the volcano plot showed the proportion of DEPs in the total identified proteins (Fig. 4A and Fig. S4E, Supplemental Digital Content 5, <http://links.lww.com/MS9/A448>). A hierarchical clustering analysis of DEPs was also performed (Fig. 4B).

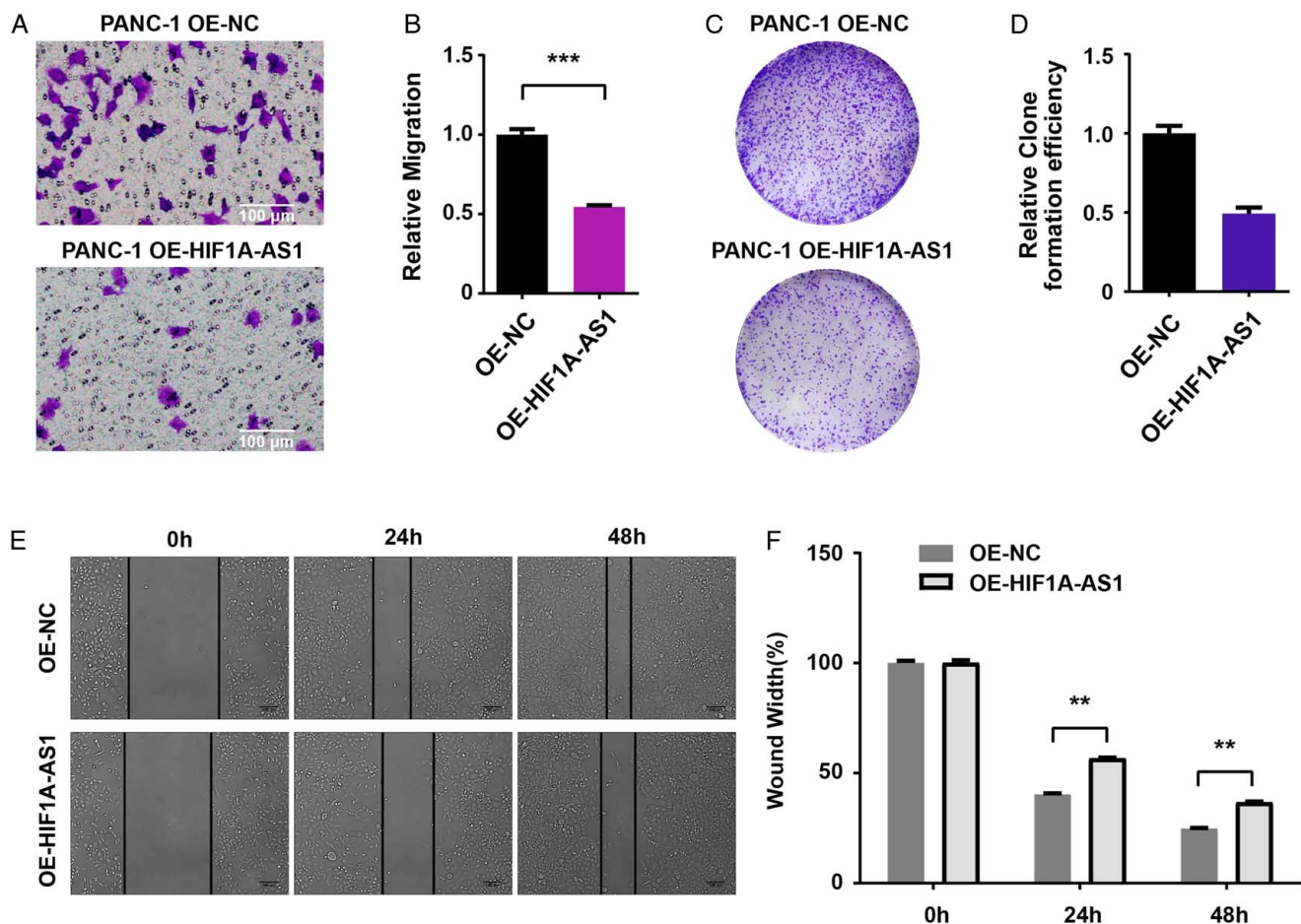


Figure 2. Overexpression (OE) of *HIF1A-AS1* regulates migration of the pancreatic cancer (PC) cells (PANC-1). (A, B) OE *HIF1A-AS1* inhibits migration of PANC-1 cells by transwell migration assay, and the properties of migration of cells were evaluated compared the NC group. (C, D) OE of *HIF1A-AS1* inhibits migration of PANC-1 cells by clone formation assays with calculating the number of colonies compared the NC group. (E, F) OE of *HIF1A-AS1* inhibits migration of PANC-1 cells by wound-healing assay at 0, 24, and 48 h post-injury time points after the wound was made with calculating the percentage of wound width compared the wound width at 0 h. ($n = 3$ cultures, paired Student's *t*-test, \pm SD) ** $P < 0.01$, *** $P < 0.001$.

In addition, KEGG enrichment for DEPs was implemented. It can be seen that the top 10 pathways were different among all up-regulated and down-regulated proteins. KEGG pathway enrichment

was also variable across the up-regulated proteins group and down-regulated proteins group. The enriched pathways for up-regulated proteins included "RNA transport" (ID: ko03013), "Metabolic

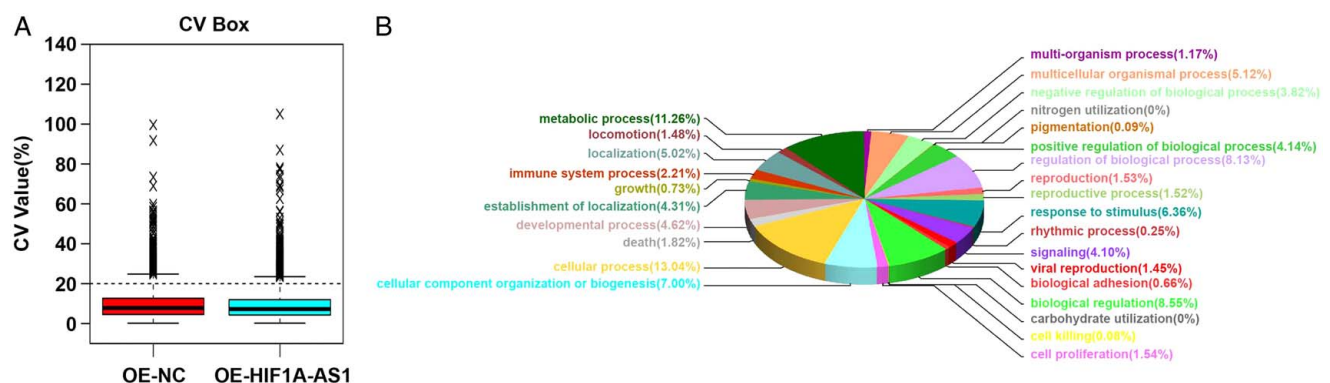


Figure 3. The summary of the isobaric tags for relative and absolute quantification (iTRAQ)-based proteomic analysis for *HIF1A-AS1* overexpression (OE) and the empty vector-controlled normal control (NC) cells groups. (A) Shows the comparison of the CV values of different experimental groups more intuitively through the CV box diagram. The box diagrams of different colours represent the CV distribution of different experimental groups. The median CV of each box from left to right is 7.81% and 7.29%, respectively. (B) GO analysis of the proportion of proteins involved in various biological processes.

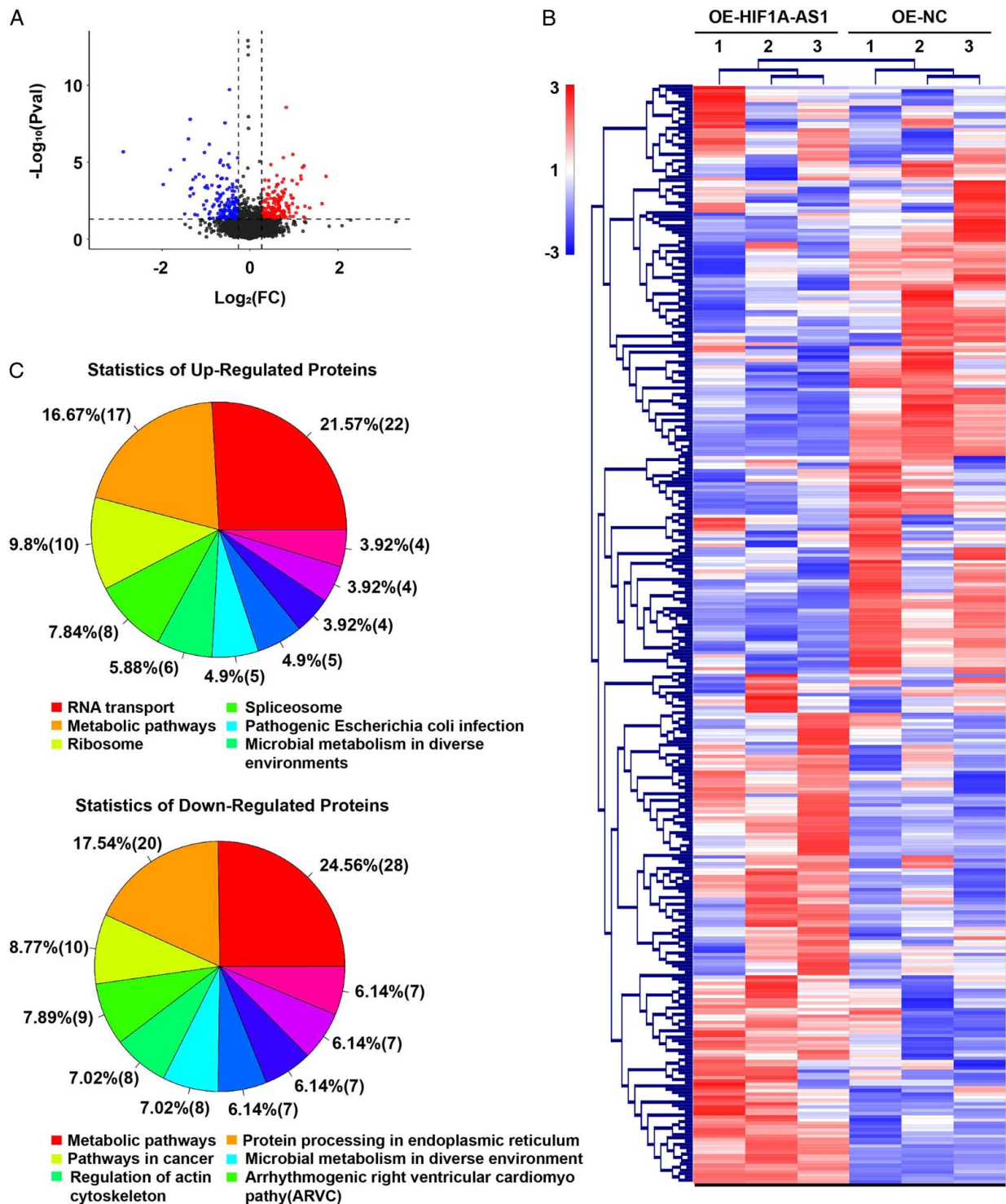


Figure 4. Exploration of differentially expressed proteins (DEPs) and functional analysis. (A) Volcano plot showing the distribution of proteins that are up-regulated (red) and down-regulated (blue) or showed no change (black) on overexpression of *HIF1A-AS1*. (B) Hierarchical clustering of proteins versus samples where rows represent the clustering of proteins, and columns represent the clustering of samples. As the protein abundance ratio changes from small to large, the heat map colour shows a corresponding blue-white-red change. (C) KEGG analysis of the proportion of proteins involved in various biological processes.

pathways” (ID: ko01100), “Ribosome” (ID: ko03010), “Spliceosome” (ID: ko03040), “Microbial metabolism in diverse environments” (ID: ko01120), “Pathogenic Escherichia coli infection” (ko05130), “Protein processing in endoplasmic reticulum”

(ko04141), “Purine metabolism” (ko00230), “Glycolysis/ Gluconeogenesis” (ko00010), “Focal adhesion” (ko04510) and so on (Table S3, Supplemental Digital Content 7, <http://links.lww.com/MS9/A450>).

Furthermore, down-regulated proteins were primarily enriched in some metabolism-related pathways and some disease-related pathways (Table S4, Supplemental Digital Content 8, <http://links.lww.com/MS9/A451>), such as “Metabolic pathways” (ID: ko01100), “Protein processing in endoplasmic reticulum” (ID: ko04141), “Pathways in cancer” (ID: ko05200), “Arrhythmogenic right ventricular cardiomyopathy” (ID: ko05412), “Microbial metabolism in diverse environments” (ID: ko01120) and “Regulation of actin cytoskeleton” (ko04810), “Tight junction” (ko04530), “Hypertrophic cardiomyopathy (HCM)” (ko05410), “Peroxisome” (ko04146), “Dilated cardiomyopathy” (ko05414) and so on (Fig. 4C).

According to these results, the excellent tumour suppressor effect of *HIF1A-AS1* may be related to its capability to regulate protein interactions, catalytic activity and enzyme regulator activity. The top 10 pathway metabolic function types were different in all up-regulated and down-regulated differential proteins by KEGG. Four types were the same containing metabolic pathway, regulation of actin cytoskeleton, microbial metabolism in diverse environments, protein processing in the endoplasmic reticulum. Pathway analysis revealed that “Metabolic pathways” at the second of up-regulated genes and at the first in down-regulated genes in the enrichment results. Moreover, OE of *HIF1A-AS1* may exhibit anticancer effects by regulating the pathways associated with metabolism of cancer. Therefore, these results suggested that *HIF1A-AS1* might affect RNA polymerase, and induce the dysfunction of metabolism and disordered proteins’ translation to control the transcription of downstream tumour-associated genes as to antagonize the proliferation, apoptosis and migration of PC cells.

Construction of DEPs protein-protein interaction (PPI) network

PPI network of common DEPs was constructed by the STRING online database and Cytoscape software to analyze the interactions of DEPs (Fig. S5, Supplemental Digital Content 9, <http://links.lww.com/MS9/A452>). A total of 338 DEPs (155 down-regulated and 183 up-regulated) were filtered into the DEPs PPI network complex. The wonderful network suggested that these DEPs might work together to regulate apoptosis, proliferation and invasion of PC cells. These proteins are expected to become targets for the treatment of PC.

Expression validation by qRT-PCR

To confirm the veracity and reliability of the proteomic assays, the expression levels of six candidate proteins were measured by qRT-qPCR, including *MX1* (Interferon-induced GTP-binding protein Mx1), *IFIH1* (Interferon-induced helicase C domain-containing protein 1), *IFIT1* (Interferon-induced protein with tetratricopeptide repeats 1), *ISG15* (Ubiquitin-like protein ISG15), *P4HB* (Protein disulfide-isomerase), *SOD2* (Superoxide dismutase [Mn], mitochondrial) (Fig. 5). Some specific primers were designed for these candidates (Table S1, Supplemental Digital Content 1,). *MX1*, *IFIH1*, *IFIT1* and *ISG15* mRNAs showed more than two-fold down-regulation as compared to NC (Fig. 5A, B, C and E) and *P4HB* more than 0.5-fold down-regulation (Fig. 5D). In addition, *SOD2* showed two-fold up-regulation (Fig. 5F). We have selected one of the genes, *ISG15*, and used antibodies to verify whether the changes in its protein expression level are consistent with the results of proteomics. The WB results revealed the protein level of *ISG15*

was down-regulated, which were consistent with the results of RT-qPCR (Fig. S1C, Supplemental Digital Content 2, <http://links.lww.com/MS9/A445>). In short, the above data supported that the results of the proteome were of credibility.

Discussion

PC remains one of the deadliest cancer types and the worlds’ most aggressive malignancies^[29]. Accumulating reports have reported the potential of lncRNAs as diagnostic or prognostic biomarkers ubiquitously dysregulated and have crucial regulatory roles in tumour cells, including PC^[30]. However, the regulatory mechanisms of multiple lncRNAs are elusive in many kinds of cancers such as thoracic aortic aneurysm and HCC. Herein, we first aimed to explore the molecular mechanism of *HIF1A-AS1* regulating PC.

From the results of proteomics, we are not sure that *HIF1A-AS1* has an effect on the expression of *HIF1A*. So in the present study, the mRNA level of *HIF1A* was slightly inhibited in *HIF1A-AS1* overexpressing groups relative to NC groups (Fig. S1D, Supplemental Digital Content 2, <http://links.lww.com/MS9/A445>). And we investigated the role of *HIF1A-AS1* on the proliferation, apoptosis, and migration of PC cells. Consistently, it was found that *HIF1A-AS1* was a suppressor of cell growth and progression in PC. Firstly, up-regulation of *HIF1A-AS1* inhibited cell growth and migration while promoting apoptosis in PANC-1 cancer cells. iTRAQ results demonstrated that *HIF1A-AS1* overexpression leads to numerous DEPs, most of which are mainly enriched in metabolism and protein translation-related pathways. In view of this, we guessed *HIF1A-AS1* mediated cell function by altering some protein translation and inducing dysfunction of metabolism in PC cells. The above is the potential molecular mechanism we guessed.

Actually, the function of *HIF1A-AS1* in other tumours has been reported. Recently, Xu and colleagues demonstrated that overexpressing *HIF1A-AS1* enhanced cell viability in pancreatic cancer cells (BXPC3 and PC1 cells). What’s more, they found *HIF1A-AS1* was up-regulated in pancreatic cancer tissues and associated with poor overall survival^[31]. Compared to normal tissues, *HIF1A-AS1* is up-regulated in some cancers, including colorectal carcinoma^[32,33] and hepatocellular carcinoma^[25]. Zhao and colleagues found inhibition of *HIF1A-AS1* promoted starvation-induced hepatocellular carcinoma cell apoptosis^[25]. The above results are inconsistent with the effect of *HIF1A-AS1* on pancreatic cancer cells in our study. In fact, this interesting phenomenon has also appeared in other RNAs or proteins. For instance, *MALAT1*, the well-studied lncRNA, was recently reported to suppress breast cancer metastasis^[34]. But in previous studies, this lncRNA generally was regarded as a promoter in many cancers, including breast cancer^[35,36], gastric cancer^[37] and ovarian cancer^[38]. *RB1* protein, the acknowledged cancer suppressor, recently was reported to prevent apoptosis in colorectal cancer^[31]. Therefore, this is an interesting phenomenon, which may be induced by individual differences. And the underlying mechanism should be explored in the future.

At last, we selected 6 DEPs (*MX1*, *IFIT1*, *IFIH1*, *P4HB*, *ISG15* and *SOD2*) for qPCR assay, and the results were consistent with the iTRAQ data, which indicated the accuracy and reliability of iTRAQ. *IFIH1* was reported to facilitate oral squamous cell carcinoma (OSCC) invasion^[39]. Recent studies have implicated *IFIH* proteins as prognostic markers to

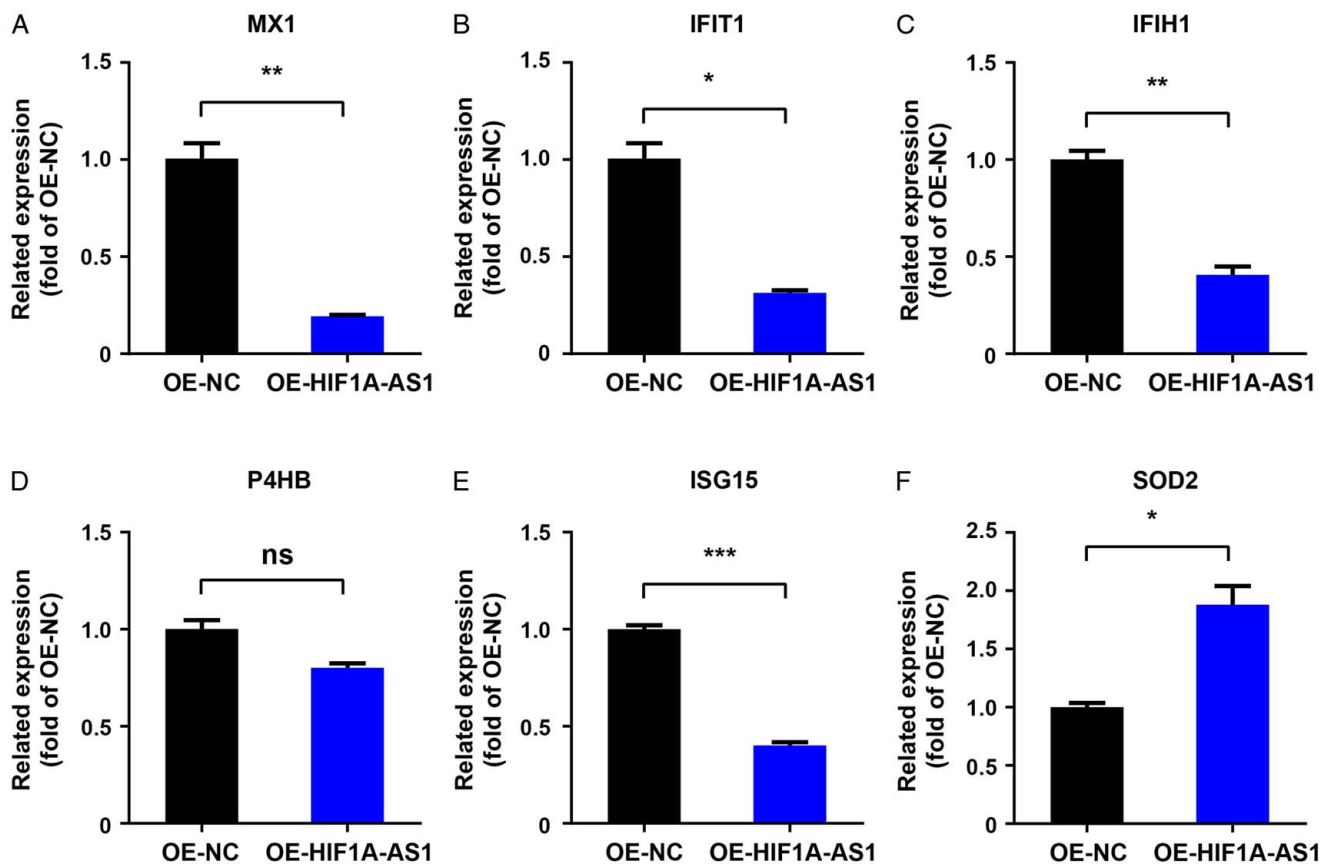


Figure 5. The quantitative real-time polymerase chain reaction (qRT-PCR) validation of some differentially expressed proteins (DEPs) obtained from isobaric tags for relative and absolute quantification (iTRAQ) analysis in Overexpression (OE) of *HIF1A-AS1* and the empty vector-controlled normal control (NC) cells groups. (A–F) The expression levels of the same DEGs including *MX1*, *IFIH1*, *IFIT1*, *P4HB*, *ISG15* and *SOD2* were validated by RT-qPCR and normalized against *Actin* expression level. Values are normalized to those from cells with control vector. $n = 3$, paired Student's *t*-test, \pm SD. * $P < 0.1$, ** $P < 0.05$, *** $P < 0.001$. *MX1*, Interferon-induced GTP-binding protein Mx1; *IFIH1*, Interferon-induced helicase C domain-containing protein 1; *IFIT1*, Interferon-induced protein with tetratricopeptide repeats 1; *ISG15*, Ubiquitin-like protein ISG15; *P4HB*, Protein disulfide-isomerase; *SOD2*, Superoxide dismutase [Mn], mitochondrial.

determine the clinical outcome of many cancers, for they wildly regulated the cell functions of many cancers^[40]. *ISG15* pathway knockdown reversed the KRAS-associated phenotypes of pancreatic ductal adenocarcinoma cells such as increased proliferation and colony formation^[41]. *ISG15* was also reported to play a vital role in regulating the growth, apoptosis or motility of other cancer cells, such as cervical cancer^[42], hepatocellular carcinoma cells^[43] and breast cancer^[44]. It has been shown that *SOD2* expression was lost in pancreatic cell lines, with the reintroduction of *SOD2* resulting in a decreased rate of proliferation^[45]. Chang *et al.*^[46] found inhibition of *SOD2* successfully enhanced migration, invasion and had poor prognosis in salivary adenoid cystic carcinoma. Knockdown of *IFIT1* effectively moderated proliferation, migration and invasion of pancreatic cancer cells via Wnt/ β -catenin pathway^[47]. Zhou *et al.*^[48] demonstrated *P4HB* knockdown promoted accumulation of reactive oxygen species (ROS), while due to the apoptosis of human colon cancer cells (HT29). Yang *et al.*^[49] found that the knockdown of *P4HB* weakened the promoting effects of *COL10A1* on cell proliferation, migration, and invasion in breast cancer. High *MX1* protein facilitated the growth of tumour and showed an association with poor patient outcomes^[50]. The above pieces of evidences demonstrated these six genes have been wildly reported to regulate the proliferation, apoptosis and migration of pancreatic

cancer cells or other cancer cells. So we guessed that these 6 DEPs played a similar role in PC cell lines (PANC-1, PATU8988 and SW1990). It should be noted that those 338 DEPs synergistically regulated the cell function of PC cells, while some of them regulated PC cells directly and others in a roundabout way. Bioinformation analysis revealed most of DEPs were enriched in metabolism and protein processing-related pathways. Hence, we believed *HIF1A-AS1* regulated cell proliferation, migration and apoptosis via inducing the dysfunction of metabolism and disordering translation of proteins.

In summary, these findings demonstrated that *HIF1A-AS1* could inhibit cell growth and progression of PANC-1 cells. In the future, studies about diagnostic specificity and sensitivity of *HIF1A-AS1*, may be used as a potential biomarker and guidance for early diagnosis of PC. Although clinical applications need to be further explored, these results further provided insight into the molecular mechanisms associated with tumorigenesis and the scientific experimental basis for the treatment of PC.

Ethical approval

The study did not involve experiments on humans or animals and did not require approval from an ethics committee.

Consent

This study does not involve personal information of patients and volunteers, nor does it use patient's medical records, so there is no corresponding supporting material.

Sources of funding

The study received no funding.

Author contribution

J.X.Z. conceived the study and drafted the manuscript, Y.F.S. participated in the data analysis, J.H.M. and X.G. participated in the experiments and manuscript revisions. All authors read and approved the final manuscript.

Conflicts of interest disclosure

The authors declare that they have no competing interests.

Research registration unique identifying number (UIN)

There is no research required for registration in this manuscript.

Guarantor

This manuscript is sponsored by Jiaxin Zhang.

Availability of data and materials

The datasets generated and/or analyzed during the current study are available in the ProteomXchange repository (Accession No: IPX0003153000). For the interview, the datasets could also be obtained from a web link: <https://www.iprox.cn/page/PSV023.html?url=1632453584186C2vO>, with a code: Nvso.

Provenance and peer review

This paper is not required and is self-delivered.

References

- [1] Kamisawa T, Wood LD, Itoi T, *et al.* Pancreatic cancer. *Lancet* 2016;388:73–85.
- [2] Torre LA, Bray F, Siegel RL, *et al.* Global cancer statistics, 2012. *CA Cancer J Clin* 2015;65:87–108.
- [3] Siegel RL, Miller KD, Jemal A. Cancer statistics, 2018. *CA Cancer J Clin* 2018;68:7–30.
- [4] Ferlay J, Soerjomataram I, Dikshit R, *et al.* Cancer incidence and mortality worldwide: sources, methods and major patterns in GLOBOCAN 2012. *Int J Cancer* 2015;136:E359–86.
- [5] Gzil A, Zarebska I, Bursiewicz W, *et al.* Markers of pancreatic cancer stem cells and their clinical and therapeutic implications. *Mol Biol Rep* 2019;46:6629–45.
- [6] Xu R, Yang J, Ren B, *et al.* Reprogramming of amino acid metabolism in pancreatic cancer: recent advances and therapeutic strategies. *Front Oncol* 2020;10:572722.
- [7] Huang X, Zhi X, Gao Y, *et al.* LncRNAs in pancreatic cancer. *Oncotarget* 2016;7:57379–90.
- [8] Duguang L, Jin H, Xiaowei Q, *et al.* The involvement of lncRNAs in the development and progression of pancreatic cancer. *Cancer Biol Ther* 2017;18:927–36.
- [9] Luo L, Wang M, Li X, *et al.* Long non-coding RNA LOC285194 in cancer. *Clin Chim Acta* 2020;502:1–8.
- [10] Guo W, Zhong K, Wei H, *et al.* Long non-coding RNA SPRY4-IT1 promotes cell proliferation and invasion by regulation of Cdc20 in pancreatic cancer cells. *PLoS One* 2018;13:e0193483.
- [11] Ding M, Fu Y, Guo F, *et al.* Long non-coding RNA MAFG-AS1 knockdown blocks malignant progression in breast cancer cells by inactivating JAK2/STAT3 signaling pathway via MAFG-AS1/miR-3196/TFAP2A axis. *Int J Clin Exp Pathol* 2020;13:2455–73.
- [12] Sanchez Calle A, Kawamura Y, Yamamoto Y, *et al.* Emerging roles of long non-coding RNA in cancer. *Cancer Sci* 2018;109:2093–100.
- [13] Tang Q, Hann SS. HOTAIR: an oncogenic long non-coding RNA in human cancer. *Cell Physiol Biochem* 2018;47:893–913.
- [14] Zhao X, Wang P, Liu J, *et al.* Gas5 exerts tumor-suppressive functions in human glioma cells by targeting miR-222. *Mol Ther* 2015;23:1899–911.
- [15] Chi Y, Wang D, Wang J, *et al.* Long non-coding RNA in the pathogenesis of cancers. *Cells* 2019;8:1015.
- [16] Qian CJ, Xu ZR, Chen LY, *et al.* LncRNA MAFG-AS1 accelerates cell migration, invasion and aerobic glycolysis of esophageal squamous cell carcinoma cells via miR-765/PDX1 axis. *Cancer Manag Res* 2020;12:6895–908.
- [17] Yang G, Lu X, Yuan L. LncRNA: a link between RNA and cancer. *Biochim Biophys Acta* 2014;1839:1097–109.
- [18] Xu J, Zhang Y, Chu L, *et al.* Long non-coding RNA HIF1A-AS1 is upregulated in intracranial aneurysms and participates in the regulation of proliferation of vascular smooth muscle cells by upregulating TGF-beta1. *Exp Ther Med* 2019;17:1797–801.
- [19] He Q, Tan J, Yu B, *et al.* Long noncoding RNA HIF1A-AS1A reduces apoptosis of vascular smooth muscle cells: implications for the pathogenesis of thoracoabdominal aorta aneurysm. *Pharmazie* 2015;70:310–5.
- [20] Wang S, Zhang X, Yuan Y, *et al.* BRG1 expression is increased in thoracic aortic aneurysms and regulates proliferation and apoptosis of vascular smooth muscle cells through the long non-coding RNA HIF1A-AS1 in vitro. *Eur J Cardiothorac Surg* 2015;47:439–46.
- [21] Wang J, Chen L, Li H, *et al.* Clopidogrel reduces apoptosis and promotes proliferation of human vascular endothelial cells induced by palmitic acid via suppression of the long non-coding RNA HIF1A-AS1 in vitro. *Mol Cell Biochem* 2015;404:203–10.
- [22] Zhang QQ, Xu MY, Qu Y, *et al.* TET3 mediates the activation of human hepatic stellate cells via modulating the expression of long non-coding RNA HIF1A-AS1. *Int J Clin Exp Pathol* 2014;7:7744–51.
- [23] Wu Y, Ding J, Sun Q, *et al.* Long noncoding RNA hypoxia-inducible factor 1 alpha-antisense RNA 1 promotes tumor necrosis factor-alpha-induced apoptosis through caspase 3 in Kupffer cells. *Medicine (Baltimore)* 2018;97:e9483.
- [24] Zhang X, Li H, Guo X, *et al.* Long noncoding RNA hypoxia-inducible factor-1 alpha-antisense RNA 1 regulates vascular smooth muscle cells to promote the development of thoracic aortic aneurysm by modulating apoptotic protease-activating factor 1 and targeting let-7g. *J Surg Res* 2020;255:602–11.
- [25] Hong F, Gao Y, Li Y, *et al.* Inhibition of HIF1A-AS1 promoted starvation-induced hepatocellular carcinoma cell apoptosis by reducing HIF-1alpha/mTOR-mediated autophagy. *World J Surg Oncol* 2020;18:113.
- [26] Cribbs AP, Kennedy A, Gregory B, *et al.* Simplified production and concentration of lentiviral vectors to achieve high transduction in primary human T cells. *BMC Biotechnol* 2013;13:98.
- [27] Livak KJ, Schmittgen TD. Analysis of relative gene expression data using real-time quantitative PCR and the 2(-Delta C(T)) Method. *Methods* 2001;25:402–8.
- [28] Mao X, Zhou L, Tey SK, *et al.* Tumour extracellular vesicle-derived Complement Factor H promotes tumorigenesis and metastasis by inhibiting complement-dependent cytotoxicity of tumour cells. *J Extracell Vesicles* 2020;10:e12031.
- [29] Ilic M, Ilic I. Epidemiology of pancreatic cancer. *World J Gastroenterol* 2016;22:9694–705.
- [30] Zhou M, Ye Z, Gu Y, *et al.* Genomic analysis of drug resistant pancreatic cancer cell line by combining long non-coding RNA and mRNA expression profiling. *Int J Clin Exp Pathol* 2015;8:38–52.
- [31] Vasaikar S, Huang C, Wang X, *et al.* Proteogenomic analysis of human colon cancer reveals new therapeutic opportunities. *Cell* 2019;177:1035–49 e1019.

- [32] Gong W, Tian M, Qiu H, *et al.* Elevated serum level of lncRNA-HIF1A-AS1 as a novel diagnostic predictor for worse prognosis in colorectal carcinoma. *Cancer Biomark* 2017;20:417–24.
- [33] Olkkonen VM, Dupree P, Killisch I, *et al.* Molecular cloning and sub-cellular localization of three GTP-binding proteins of the rab subfamily. *Journal of Cell Science* 1993;106:1249–61.
- [34] Kim J, Piao HL, Kim BJ, *et al.* Long noncoding RNA MALAT1 suppresses breast cancer metastasis. *Nat Genet* 2018;50:1705–15.
- [35] Chou J, Wang B, Zheng T, *et al.* MALAT1 induced migration and invasion of human breast cancer cells by competitively binding miR-1 with cdc42. *Biochem Biophys Res Commun* 2016;472:262–9.
- [36] Zuo Y, Li Y, Zhou Z, *et al.* Long non-coding RNA MALAT1 promotes proliferation and invasion via targeting miR-129-5p in triple-negative breast cancer. *Biomed Pharmacother* 2017;95:922–8.
- [37] Li Y, Wu Z, Yuan J, *et al.* Long non-coding RNA MALAT1 promotes gastric cancer tumorigenicity and metastasis by regulating vasculogenic mimicry and angiogenesis. *Cancer Lett* 2017;395:31–44.
- [38] Gordon MA, Babbs B, Cochrane DR, *et al.* The long non-coding RNA MALAT1 promotes ovarian cancer progression by regulating RBFOX2-mediated alternative splicing. *Mol Carcinog* 2019;58:196–205.
- [39] Pidugu VK, Wu MM, Yen AH, *et al.* IFIT1 and IFIT3 promote oral squamous cell carcinoma metastasis and contribute to the anti-tumor effect of gefitinib via enhancing p-EGFR recycling. *Oncogene* 2019;38:3232–47.
- [40] Pidugu VK, Pidugu HB, Wu MM, *et al.* Emerging functions of human IFIT proteins in cancer. *Front Mol Biosci* 2019;6:148.
- [41] Burks J, Fleury A, Livingston S, *et al.* ISG15 pathway knockdown reverses pancreatic cancer cell transformation and decreases murine pancreatic tumor growth via downregulation of PDL-1 expression. *Cancer Immunol Immunother* 2019;68:2029–39.
- [42] Zhou MJ, Chen FZ, Chen HC, *et al.* ISG15 inhibits cancer cell growth and promotes apoptosis. *Int J Mol Med* 2017;39:446–52.
- [43] Liu Z, Ma M, Yan L, *et al.* miR-370 regulates ISG15 expression and influences IFN-alpha sensitivity in hepatocellular carcinoma cells. *Cancer Biomark* 2018;22:453–66.
- [44] Kariri YA, Alsaleem M, Joseph C, *et al.* The prognostic significance of interferon-stimulated gene 15 (ISG15) in invasive breast cancer. *Breast Cancer Res Treat* 2021;185:293–305.
- [45] Hurt EM, Thomas SB, Peng B, *et al.* Molecular consequences of SOD2 expression in epigenetically silenced pancreatic carcinoma cell lines. *Br J Cancer* 2007;97:1116–23.
- [46] Chang B, Yang H, Jiao Y, *et al.* SOD2 deregulation enhances migration, invasion and has poor prognosis in salivary adenoid cystic carcinoma. *Sci Rep* 2016;6:25918.
- [47] Li TH, Zhao BB, Qin C, *et al.* IFIT1 modulates the proliferation, migration and invasion of pancreatic cancer cells via Wnt/beta-catenin signaling. *Cell Oncol (Dordr)* 2021;44:1425–37.
- [48] Zhou Y, Yang J, Zhang Q, *et al.* P4HB knockdown induces human HT29 colon cancer cell apoptosis through the generation of reactive oxygen species and inactivation of STAT3 signaling. *Mol Med Rep* 2019;19:231–7.
- [49] Yang W, Wu X, Zhou F. Collagen type X alpha 1 (COL10A1) contributes to cell proliferation, migration, and invasion by targeting prolyl 4-hydroxylase beta polypeptide (P4HB) in breast cancer. *Med Sci Monit* 2021;27:e928919.
- [50] Aljohani AI, Joseph C, Kurozumi S, *et al.* Myxovirus resistance 1 (MX1) is an independent predictor of poor outcome in invasive breast cancer. *Breast Cancer Res Treat* 2020;181:541–51.